 doi:10.20944/preprints202101.0185.v1

Article

Combined Linkage Analysis and Genome-wide Association Study Reveal QTLs and Candidate Genes Conferring Genetic Control of Prolificacy Trait in Maize

Zhao Wang[1#], Jingyang Gao[1#], Yunmeng Li[1], Razia sultana Jemim[2], Yifan Luan[1], Cong Mu[1], Yunxia Song[1], Chaopei Dong[1], Jing Xu[1], Zhaokun Wu[1], Wenchao Ye[2], Huan Li[2], Jiafa Chen[2], Haidong Yu[2], Zijian Zhou[2*] and Jianyu Wu[1*]

[1] Affiliation 1; College of Agronomy, Henan Agricultural University, Zhengzhou, 450002, China.
[2] Affiliation 2; College of Life Sciences, Synergetic Innovation Center of Henan Grain Crops and National Key Laboratory of Wheat and Maize Crop Science, Henan Agricultural University, Zhengzhou 450002, China.
# These two authors contributed equally to this work.
* Correspondence: Zijian Zhou (zhouzijian19900601@163.com); Jianyu Wu (wujianyu40@126.com).

Abstract: For the different harvest targets, the requirement for the prolificacy trait of maize was also different, so prolificacy is of great significance for modern production. Although some QTLs and genes associated with prolificacy in teosinte have been reported, the genetic mechanism of prolificacy in maize has not been fully elucidated. In this study, two RIL populations and GWAS population were used to genetic research of prolificacy trait in maize, with multi-environment. Combine linkage analysis and Genome-wide association study has identified a total of 13 QTLs and 8 significant SNPs. There were two genes related to tissue differentiation in the stable QTL *qP9-2*, and two significant SNPs corresponding to three genes were in QTL *qP5-1* and QTL *qP7-1*, respectively. Four candidate genes *GRMZM2G317262*, *GRMZM2G317584*, *GRMZM5G882364* and *GRMZM2G141679* were finally screened out by qRT-PCR analysis. Based on the function of candidate genes, ethylene signaling pathway plays an important role in the formation of prolificacy in maize. It has deepened our understanding of the formation mechanism of prolificacy and laid a foundation for breeding new varieties with various prolificacy in maize.

Keywords: Maize; Prolificacy; Linkage analysis; GWAS; Candidate genes; Ethylene signaling

1. Introduction

Maize (Zea mays L.) is one of the world's staple food and industrial raw materials and energy crops [1]. In maize genetics and breeding, the number of ears on a plant is scored as prolificacy [2]. Yield which consists of the ear number per plant and the yield per ear is the goal of the ordinary maize. Prolificacy makes dominant ears smaller and produces invalid ears, which leads to lower yield [3]. However, the economic benefits of special maize such as silage corn, baby corn and sweet corn are closely related to the number of ears [4,5]. In addition, for genetic breeding, maize inbred lines with prolificacy can amplify the events of hybrid combinations. Therefore, it is very important to study the prolificacy trait in maize.

Typically, maize has 1-2 economic benefits ears, with only one single ear at each node. The prolificacy is that maize has 3 or more ears, including multi-node prolificacy, single-node prolificacy and multi-tiller prolificacy. Maize originated from a single domestication event of teosinte in the Balsas River Basin, Mexico, as early as 9000 years ago [6,7]. During the process of maize evolution and artificial selection, the tiller and prolificacy characters of maize gradually degenerate [7,8]. But under certain environmental conditions, the tillering and prolificacy phenomenon of maize still occurs. Besides, axillary buds can potentially develop at every node except the top 5-9 nodes below the tassel [9]. Interestingly, the ear of maize belongs to an abnormal stem, and axillary meristem in

Preprints (www.preprints.org) | NOT PEER-REVIEWED | Posted: 11 January 2021 doi:10.20944/preprints202101.0185.v1

underground will develop into tillers, while that in aboveground may develop into ears. The phenomenon of apical dominance plays an important role in regulating, in which the growing apex meristem produces a long-distance inhibitory to maintain axillary buds in a dormant state axillary shoots [10]. Dormancy is tightly regulated by a complex interaction between internal and external stimuli[11]. When maize suffers high-temperature stress, diseases and insect pests, high density, or not timely pollination, the development of dominant ears is hindered, leading to the reduction of apex dominance [12]. Then, lower axillary buds develop further to form prolificacy. Besides, the upper internode of some tropical lines which grow in temperate regions, elongate slowly, and the lower axillary buds develop preferentially, which can form prolificacy. Adequate nutrients, such as increased use of nitrogen fertilizer, will also lead to the prolificacy by promoting lower axillary meristems growth [13].

Phytohormone plays an important role in the growth and development of the female panicle, among which auxin is the main plant hormone to maintain and remove apical dominance. The polar transport of auxin will affect the development of ears and lower axillary buds. Studies have shown that the regulation of auxin responses began at the initial stage of ear development [14]. Arabidopsis regulates the development of apical and basal boundaries in octagonal tissues through positive regulation of 'mid-level' auxin responses [15]. Various studies revealed antagonistic interactions between the plant hormones auxin and cytokinin (CK) in regulating bud outgrowth[16,17]. Studies in other plant species also showed that auxin and abscisic acid (ABA) inhibited bud growth, while cytokinin promoted it [18,19]. Strigolactones (SLs) and gibberellin (GA) can repress bud outgrowth while brassinosteroids (BRs) promote bud outgrowth in rice [19]. Ethylene participates in ear development and plays a negative regulatory role in the early stage of ear development [14]. Because of a strong carbohydrate requirement in dividing and differentiating cells, it makes sense that meristem maintenance, identity, and organogenesis should be carefully coordinated with nutrient status [20]. There is also increasing evidence that sugars can regulate specific developmental programs and transitions via genes that control meristem maintenance and identity [21,22]. Plasticity in plant development is controlled by environmental signals with largely unknown signalling networks. In particular, the maize G protein signaling plays a key role in ear development and prolificacy [23].

Prolificacy is a result of several factors such as initiation of axillary primordia, development of axillary bud, branch elongation, ear development and female floret development, which in turn are controlled by a large number of genes [24]. The quantitative inheritance pattern of prolificacy with the prevalence of non-allelic interactions of duplicate epistasis type has been observed. Dominance × dominance effect was predominant over additive × additive and additive × dominance effect [24]. Since the multi-ear traits of maize are derived from teosinte, QTLs and related genes controlling the multi-ear traits can be found through genetic research on the hybrid offspring of teosinte and maize inbred line. Some QTLs associated with maize prolificacy traits have been identified. Eight QTLs were identified which were associated with maize prolificacy, one QTL (*prol1.1*) is located on the short arm of chromosome 1 and accounts for 36.7% of the phenotypic variance, which has a much larger effect than the other seven. Fine-mapped *prol1.1* to a 2.7 kb ''causative region'' upstream of the grassy tillers1 (*gt1*) gene, which encodes a homeodomain leucine zipper transcription factor [2]. The *grassy tillers1* (*gt1*) is named for excessive tillering and plays a role in maize development [25]. Loss of the gt1 function alleles also cause trait changes including prolificacy in maize [2]. *Teosinte branched1* (*tb1*) is responsible for the shortening and feminization of the axillary branches in domesticated maize [26,27]. Since both tillers (basal lateral branches) and upper lateral branches arise from axillary meristems, in a general sense, *tb1* governs the fate of the axillary meristems [28].

Although the genetic mechanism of the prolificacy trait has been elucidated by the genetic populations of maize and teosinte, the genetic basis of the prolificacy among modern maize inbred lines has not been revealed in detail. In this study, two RIL popu-

 doi:10.20944/preprints202101.0185.v1

lations and GWAS population used to identify the QTLs and candidate genes associated with prolificacy trait in maize. Specifically, the three aims of this investigation were to (1) identify the stable QTLs of prolificacy trait, (2) identify key candidate genes, (3) analyze the genetic mechanism of prolificacy in maize.

2. Results

2.1. Phenotypic analysis

Through the investigation of prolificacy traits in different environments of three populations, we analyzed the phenotypic frequency of each environment. The phenotypic distribution of each environment is similar to the normal distribution (Figure 1), indicating that the prolificacy of maize is a quantitative trait controlled by multiple genes. Besides, phenotypes in different environments in the three populations were correlated, indicating that phenotypic data structures in different environments were relatively similar, and joint analysis of phenotypic data in multiple environments in the population could be conducted.

Preprints (www.preprints.org) | NOT PEER-REVIEWED | Posted: 11 January 2021 doi:10.20944/preprints202101.0185.v1

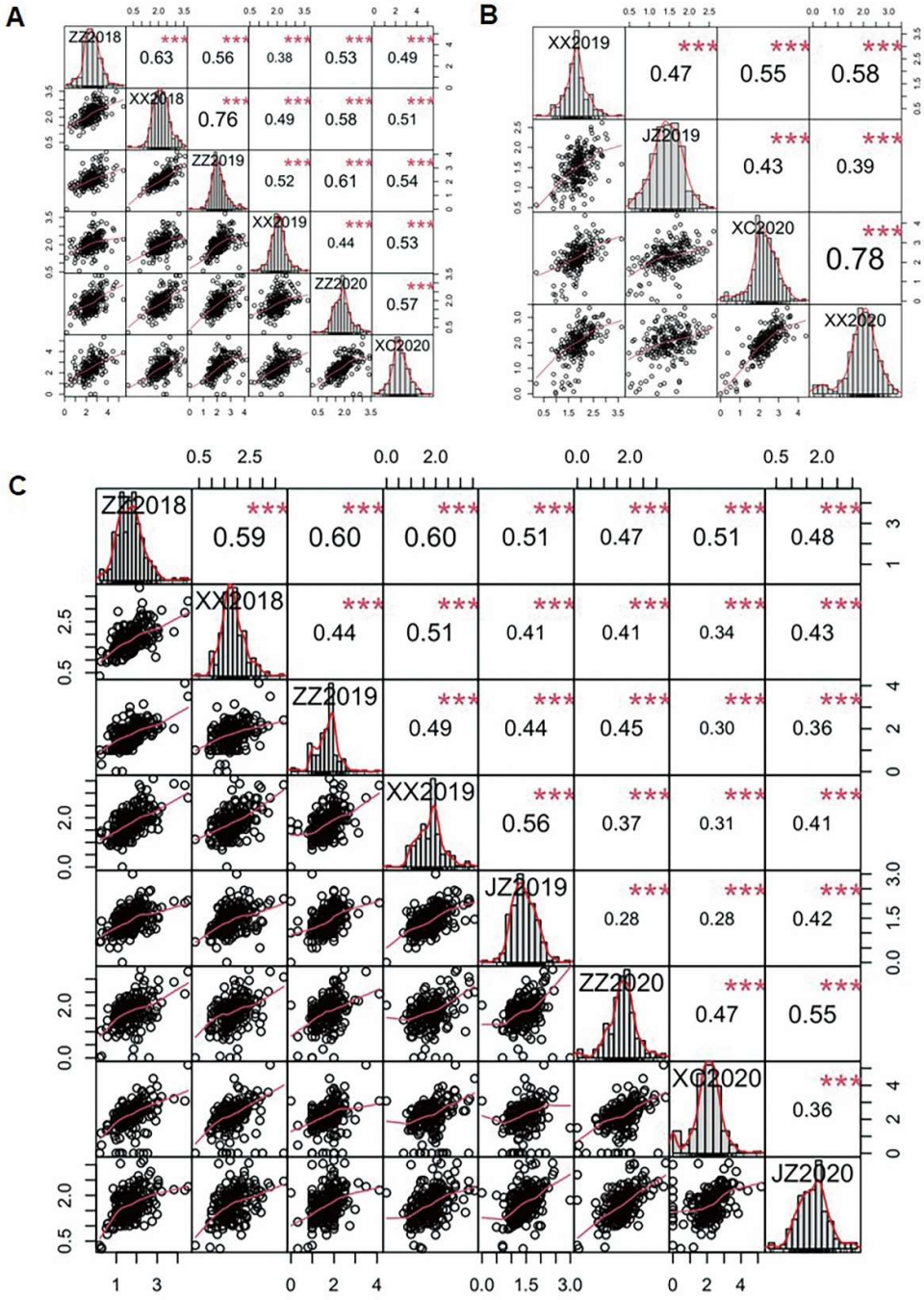

Figure 1 **Frequency distribution histogram and correlation analysis of three populations.** A: BT-1×XI502 RIL population. B: N6×CML170 RIL population. C: GWAS population. Regression Plot, histograms and Pearson correlation coefficients (P=0.01) for prolificacy trait among different environments (ZZ, Zhengzhou; XX, Xunxian; JZ, Jiaozuo; XC, Xuchang). The diagonal of the figure is the frequency distribution histogram of each environment, and the bottom left is the phenotypic scatter diagram, in which ○ and ● represent the two different environments. On the upper right is the correlation coefficient, with the ***representing a significant correlation.

Preprints (www.preprints.org) | NOT PEER-REVIEWED | Posted: 11 January 2021 doi:10.20944/preprints202101.0185.v1

In order to further dissect the phenotypic variation of prolificacy traits, we implemented heritability analysis in three populations respectively (Table 1). The combined heritability of each population was 0.87, 0.83, and 0.85, respectively. This indicates that the prolificacy traits are mainly controlled by genetics.

Table 1. Variances and heritabilities of prolificacy in three maize populations.

Population	Environment	DF	σ_g^2	σ_{ge}^2	σ_e^2	H^2
BT-1×XI502 RIL	ZZ2018	226	0.50		0.29	0.76
	XX2018	232	0.23		0.16	0.74
	ZZ2019	247	0.22		0.16	0.75
	XX2019	254	0.12		0.18	0.61
	ZZ2020	252	0.21		0.10	0.81
	XC2020	238	0.47		0.34	0.73
	BLUE	1449	0.20	0.09	0.26	0.87
N6×CML170 RIL	XX2019	230	0.17		0.10	0.78
	JZ2019	233	0.09		0.15	0.55
	XC2020	224	0.41		0.15	0.85
	XX2020	233	0.35		0.05	0.93
	BLUE	920	0.18	0.09	0.21	0.83
GWAS	ZZ2018	205	0.39		0.12	0.86
	XX2018	202	0.14		0.21	0.55
	XX2019	215	0.19		0.18	0.70
	JZ2019	209	0.08		0.15	0.51
	ZZ2020	190	0.24		0.16	0.72
	XC2020	165	0.54		0.36	0.71
	JZ2020	199	0.18		0.15	0.68
	BLUE	1385	0.15	0.09	0.23	0.85

2.2. Linkage analysis

The genetic maps of two RIL populations (BT×XI502 RIL and N6×CML170 RIL) were constructed (figure S1). There were 7,528 polymorphic SNP markers in the BT-1×XI502 RIL population, with a total length of 2541cM and an average genetic distance of 0.34cM between the markers. In the N6×CML170 RIL population, there were 3998 polymorphic SNP markers with a total length of 1450.13cM and an average genetic distance of 0.36cM between the markers.

The linkage analysis of the RIL population was carried out by composite interval mapping method. Firstly, QTL analysis was performed on prolific phenotypes in different environments. 30 and 11 QTLs were identified by the two populations respectively (Table S2 and Table S3). In addition, we performed combined analysis of multiple environments for RIL populations with the best linear unbiased estimate (BLUE) (Table 2). A total of 13 QTLs were identified on chromosomes 1, 2, 5, 6, 7, 9 and 10 by the two RIL populations. One of these QTLs *qP6-1* on chromosome 6 in the BT-1×XI502 RIL explained the highest phenotypic variation, 7.65%, and the QTL *qP9-3* on chromosome 9 in the N6×CML170 RIL explained the highest, 7.69%. It is noteworthy that both two populations detected the common QTL on chromosome 9, *qP9-2* and *qP9-3*. The overlapping interval of two QTLs will be an important object of our study. A total of 15 genes were identified in the overlapping interval 9_135605559 to 9_136357845 (Table 3). Two of fifteen genes

Preprints (www.preprints.org) | NOT PEER-REVIEWED | Posted: 11 January 2021 doi:10.20944/preprints202101.0185.v1

have been reported associated with tissue differentiation. The gene *GRMZM2G317262* encoding the F-box family protein, and *GRMZM2G317584* encoding Ethylene insensitive 3 family protein.

Table 2. Quantitative trait loci for maize prolificacy in two RIL populations.

Trait Name	Chromosome	QTL Name	Left Marker	Right Marker	LOD	PVE(%)	Add
BT-1×XI502 Population	1	*qP1-1*	1_270460620	1_270866951	4.06	4.37	0.08
	2	*qP2-1*	2_6635220	2_6961027	6.84	7.63	-0.11
	2	*qP2-2*	2_238895013	2_239263725	3.09	3.42	-0.08
	6	*qP6-1*	6_97446909	6_97774642	6.95	7.65	-0.11
	7	*qP7-1*	7_103651052	7_106918613	2.94	3.33	-0.07
	9	*qP9-1*	9_4771111	9_4987736	3.46	3.86	0.08
	9	*qP9-2*	9_135605559	9_136370952	3.81	4.18	-0.08
N6×CML170 Population	1	*qP1-2*	201510283	202298178	3.93	3.27	-0.10
	1	*qP1-3*	22965625	24963234	7.44	6.56	0.14
	2	*qP2-3*	49009196	49720987	3.31	2.76	-0.10
	5	*qP5-1*	181268715	182051176	3.29	2.79	-0.09
	9	*qP9-3*	135295686	136357845	8.40	7.69	0.15
	10	*qP10-1*	142077552	142161845	2.70	2.23	0.08

Table 3. Candidate genes and their functional annotations in *qP9-2*.

Gene	Annotation
GRMZM2G131785	ABC transporter ATP-binding protein
GRMZM5G872256	glycosyl transferase 8 domain containing protein
GRMZM5G862107	(ARRPS1, RPS1) ribosomal protein S1
GRMZM2G134279	MYB family transcription factor
GRMZM2G060842	expressed protein
GRMZM2G060918	(AtWRKY41, WRKY41) WRKY family transcription factor
GRMZM2G317262	OsFBX82 - F-box domain containing protein
GRMZM2G317267	none
GRMZM2G161664	Leucine-rich receptor-like protein kinase family protein
GRMZM2G014839	(ATCAMBP25, CAMBP25) calmodulin (CAM)-binding protein of 25 kDa
GRMZM2G704475	(ATECP63, ECP63) embryonic cell protein 63
GRMZM2G043983	(TOM40) translocase of the outer mitochondrial membrane
AC207454.3_FG004	none
GRMZM2G317584	(AtEIN3, EIN3) Ethylene insensitive 3 family protein
GRMZM2G022398	exostosin family domain containing protein

2.3 Genome-wide association study

Preprints (www.preprints.org) | NOT PEER-REVIEWED | Posted: 11 January 2021 doi:10.20944/preprints202101.0185.v1

In short, the GWAS population was constructed by three subgroups. The largest subgroup 1 contained tropical germplasm available at CIMMYT. Tangsipingtou heterotic subpopulation generated from Chinese very important elite materials belonged to subgroup 2, and most of the lines in Subgroup 3 were from the Chinese Reid and Lancaster heterotic subpopulation. Genome-wide association study is carried out for a single environment (figure S2 and S3). A total of 106 Significant SNPs were detected, which correspond to 186 genes, (Table S4).

Through the joint analysis of the phenotypes in 8 environments of the GWAS population (Figure 2). A total of 8 significant SNPs were detected, which were located on chromosome 1, 5, 6 and 7, respectively. The most significant SNP site was S6_31649694 on chromosome 6. According to the LD value (10-20kb) of the GWAS population, we identified 7 candidate genes (Table 4). *GRMZM2G025959*, *GRMZM2G088736*, *GRMZM5G882364*, *GRMZM2G141679*, *GRMZM2G109126*, *GRMZM2G046297* and *GRMZM5G801004*. By comparing to the QTL, the associated SNPs of S5_178621021 were localized in the interval of QTL *qP5-1*. The two corresponding genes *GRMZM2G088736* and *GRMZM5G882364* were identified based on the MaizeGDB database (http://www.maizegdb.org/), which encodes an ycf45 protein and Copper transport protein, respectively. The SNP S7_100241083 was localized in the interval of QTL *qP7-1*. The corresponding gene *GRMZM2G141679* encodes an ethylene-responsive transcription factor. So, the genes *GRMZM2G088736*, *GRMZM5G882364* and *GRMZM2G141679*, were considered important candidate genes.

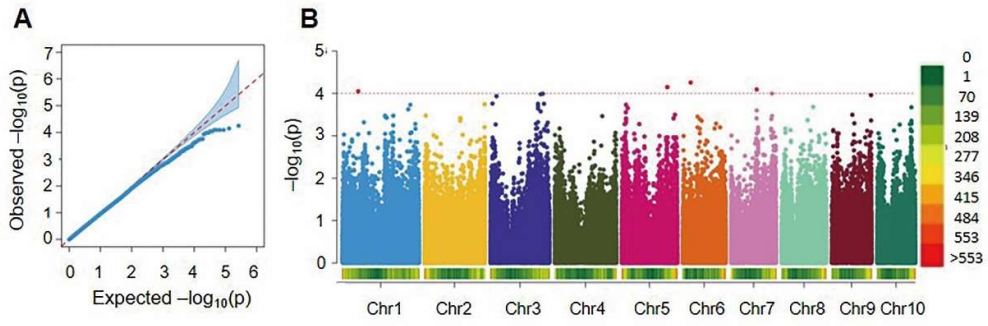

Figure 2. QQ-plots and Manhattan plots of GWAS for the maize prolificacy.

A: QQ-plots. B: Manhattan plots. Plots above the imaginary line show the genome-wide significance with threshold of - log (10^{-4}). The horizontal axis shows the SNP density of physical positions on the ten chromosomes. The vertical axis shows the value of - log (P).

Table 4. The significant SNPs and their candidate genes associated with maize prolificacy identified in the GWAS with p-value less than 10^{-4}.

Chromosome	Marker	P	R^2	Gene	Annotation
6	S6_33143794	5.58E-05	0.093	*GRMZM2G025959*	Mannose-binding lectin superfamily protein

Preprints (www.preprints.org) | NOT PEER-REVIEWED | Posted: 11 January 2021 doi:10.20944/preprints202101.0185.v1

					Jacalin-like lectin domain containing protein
5	S5_182703041	7.07E-05	0.075	*GRMZM2G088736* *GRMZM5G882364*	(ATCUL4, CUL4) cullin4 uncharacterized protein ycf45 Copper transport protein family heavy metal transport/detoxification protein
7	S7_103378110 S7_103378111 S7_103378116 S7_103378120	8.05E-05 8.05E-05 8.05E-05 8.05E-05	0.074 0.074 0.074 0.074	*GRMZM2G141679*	Integrase-type DNA-binding superfamily protein ethylene-responsive transcription factor
1	S1_63928493 S1_63928503	8.91E-05 8.93E-05	0.083 0.081	*GRMZM2G109126* *GRMZM2G046297* *GRMZM5G801004*	none Protein kinase superfamily protein tyrosine protein kinase domain containing protein none

2.4 Quantitative analysis

In summary, five important candidate genes were selected, namely, *GRMZM2G317262*, *GRMZM2G317584*, *GRMZM2G088736*, *GRMZM5G882364* and *GRMZM2G141679*. In order to screen and verify the potential candidate genes, the relative expression levels of the above five genes were measured (Figure 3). The gene *GRMZM2G088736* was found not to be expressed in different parents and different internodes. The expression level of N1 ear in BT-1 was used as a calibrator to analyze the gene expression of candidate genes. The expression level of candidate gene *GRMZM2G141679* was different between different nodes, and showed an upward trend, except for the XI502 inbred line. The expression of gene *GRMZM2G317584* in the four inbred lines showed an increasing trend with the decrease of ear position. The expression of these two genes was related to the differentiation of the young ear in maize and positively regulated the development of the ear. The expression level of *GRMZM2G317262* in different internodes of the four inbred lines were relatively stable, and it was obvious that the gene *GRMZM2G141679* and *GRMZM2G317262* expression levels of multi-ear inbred lines XI502 and CML170 were lower than those in the low-ear inbred lines BT-1 and N6. The expression level of gene *GRMZM5G882364* was not significantly different in the female panicle between different nodes, and between the four inbred lines.

Preprints (www.preprints.org) | NOT PEER-REVIEWED | Posted: 11 January 2021 doi:10.20944/preprints202101.0185.v1

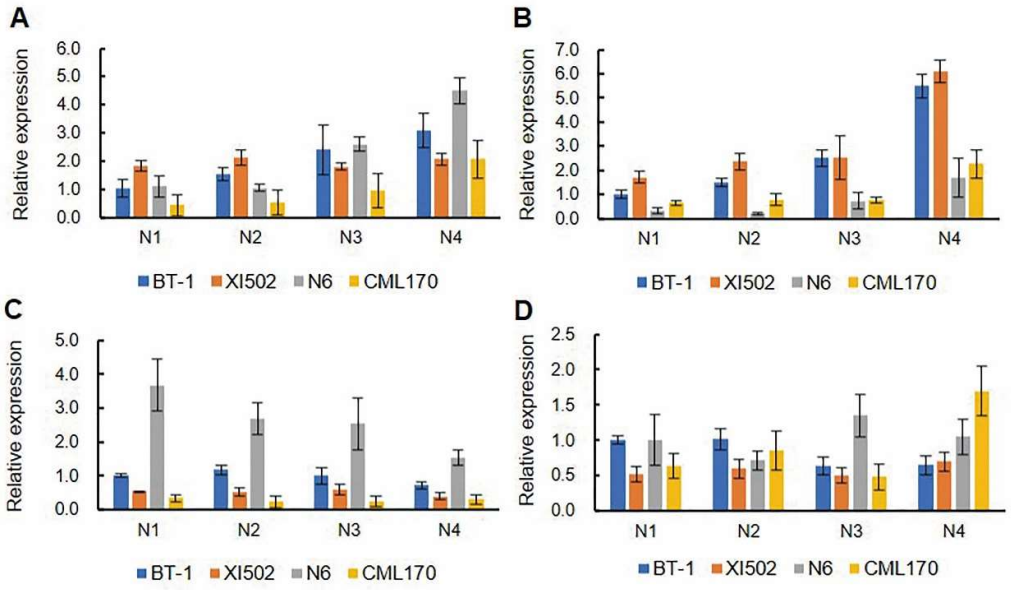

Figure 3. The relative expression of candidate genes. A: *GRMZM2G141679*. B: *GRMZM2G317584*. C: *GRMZM2G317262*. D: *GRMZM5G882364*.

3. Discussion

The development of maize ear is divided into four stages, namely, growth cone extension stage, spikelet differentiation stage, floret differentiation stage and sex organ formation stage [29]. Usually, the axillary buds of the middle and lower part of maize stay in the early stage of ear development, and only 1-2 axillary buds of the middle and upper part of maize will develop to ear. The differentiation process of the ear in maize is similar to the tassel, but the ear differentiates is late and quickly. Finally, the silk of the ear receives the pollen and develops the mature ear. The silking of the ear with different development of axillary buds can be taken as the criterion for the formation of multiple ears of maize, which had a long period and easily recognized. There is apical dominance in ear development of maize. When the dominant ear of maize is subjected to biological or abiotic stress, growth and development are hindered and apical dominance is weakened, which promotes the development of lower female ear and finally effects prolificacy trait. In abiotic stress, high temperature is a key factor affecting plant growth and development. Prolificacy can indirectly reflect the high temperature tolerance of dominant ear in maize [30]. Therefore, it is very important to analyze the genetic mechanism of maize high temperature tolerance from the perspective of prolificacy.

Through QTL analysis, 13 QTLs affecting prolificacy trait were identified, among which the range of *qP1-3* (V4: 22,965,625-24,963,234) includes the *prol1.1* (V4: 23,005,166-23,462,365) and *gt1*. QTL *qP9-2* and *qP9-3* located on chromosome 9 were multi-environment and multi-population stable QTLs, of which including 15 genes in the overlapping interval from 9_135605559 to 9_136357845. Combined with functional annotation, two candidate genes, *GRMZM2G317262* and *GRMZM2G317584* were selected. Through the Genome-wide association study, 8 significant SNPs were identified, corresponding to 7 candidate genes. Three of seven candidate genes, *GRMZM2G141679*, *GRMZM2G088736* and *GRMZM5G882364*, were selected combined linkage analysis results. Further expression analysis initially studied the functions of the above five candidate genes, and the results showed that *GRMZM2G317262*, *GRMZM2G317584*, *GRMZM2G141679* and *GRMZM5G882364* may be associated with maize prolificacy traits.

 doi:10.20944/preprints202101.0185.v1

Hormones play an important role in the growth and development of plants, among which auxin, gibberellin, cytokinin and BRs promote growth, while abscisic acid and ethylene play the opposite role. Candidate gene *GRMZM2G317584* identified by linkage analysis encodes an ethylene-insensitive3 protein (EIN3/EIL). Ethylene-insensitive3 (EIN3/EIL) is a key regulator for initiation of ethylene-mediated downstream transcriptional cascades by binding to primary ethylene response elements (PEREs) and EIL conserved binding sequences (ECBSs) in the promoters of downstream genes involved in the ethylene reaction [31,32]. EIL is an important gene family in plants and plays key roles in the ethylene signaling pathway which regulates a broad spectrum of plant growth and development, as well as defenses to various biological and abiotic stresses [33]. Previous studies have shown that ethylene has a negative regulatory effect on the early ear development of maize[14]. Ethylene regulates the responses of plants to various abiotic stresses, especially in low temperature stress [34]. Ethylene biosynthesis and signaling negatively regulate plant freezing tolerance by repressing the cold-inducible CBFs and type-A ARR genes in Arabidopsis [35].

GRMZM2G141679 identified by Genome Wide Association Study encodes an ethylene-responsive transcription factor. Quantitative analysis showed that the expression level of *GRMZM2G141679* was higher in the early stage of ear development and lower in the prolific parents, indicating that this gene may negatively regulate the occurrence of the prolificacy trait. The expression level of *GRMZM2G317584* is higher in early ear development, indicating that the gene plays an important role in early ear development.

The gene *GRMZM2G317262* encodes an F-box family protein. The F-box family protein is involved in the regulation of various developmental processes in plants, such as photomorphogenesis, circadian clock regulation, self-incompatibility, anther meristem and floral organ identity determination, etc. It is reported that the F-box gene (GenBank ID: AJ577363) was expressed during all the spike developmental stages in wheat [36]. F-box proteins contain a conserved F-box domain, which interacts with Skp1, CULLIN, and RBX1 to form the SCF complex [37]. The SCF complexes confer the specificity of selective protein ubiquitination and subsequent degradation by the 26S proteasome [38]. Meanwhile, ethylene - induced stability of EIN3/EIL1 is mediated by proteasomal degradation of two F-box proteins [35,39]. Based on the quantitative analysis of gene *GRMZM2G317262*, it can be seen that the expression level of this gene is relatively low in the early ear development and in the high prolificacy parent, which indicated that the gene *GRMZM2G317262* negatively regulated prolificacy trait.

The gene *GRMZM5G882364* encoding the Copper transport protein family. Copper is an essential metal for plants. It plays key roles in photosynthetic and respiratory electron transport chains, in ethylene sensing, cell wall metabolism, oxidative stress protection and biogenesis of molybdenum cofactor. Cu homeostasis is also receiving a growing interest in plant research, since it is implicated in adaptive responses to the oxidative damage produced by environmental stress [40]. The ethylene receptor ETR1, which localizes in the endoplasmic reticulum (ER), high affinity binding of ethylene is mediated by a copper co-factor [41].

Since the functions of the four candidate genes are related to ethylene metabolic pathways, the model was speculated, (Figure 4). Under normal circumstances, the expression level of ethylene transcription factor is low in-ear (N1 and N2), the key of the ethylene downstream cascade control factor of EIN3 expression level is low, at the same time, the expression of F-box makes EIN3 unstable, causing the low ethylene content in the ear (N1 and N2). It weakens ethylene to continue the metabolism of the binding copper ions ethylene receptor ETR1 in the endoplasmic reticulum, causing ear (N1 and N2) normal growth. After the high-temperature stress, the influx of copper ions increased, and the ethylene receptor ETR1 increased in the endoplasmic reticulum. It may be that the expression of F-box protein decreased, leading to the structural stability of EIN3, which in turn led to the enhancement of ethylene metabolism pathway, and finally inhibited the development of ear (N1 and N2), promoted the development of ear (N3 and N4), and formed prolificacy trait.

Preprints (www.preprints.org) | NOT PEER-REVIEWED | Posted: 11 January 2021 doi:10.20944/preprints202101.0185.v1

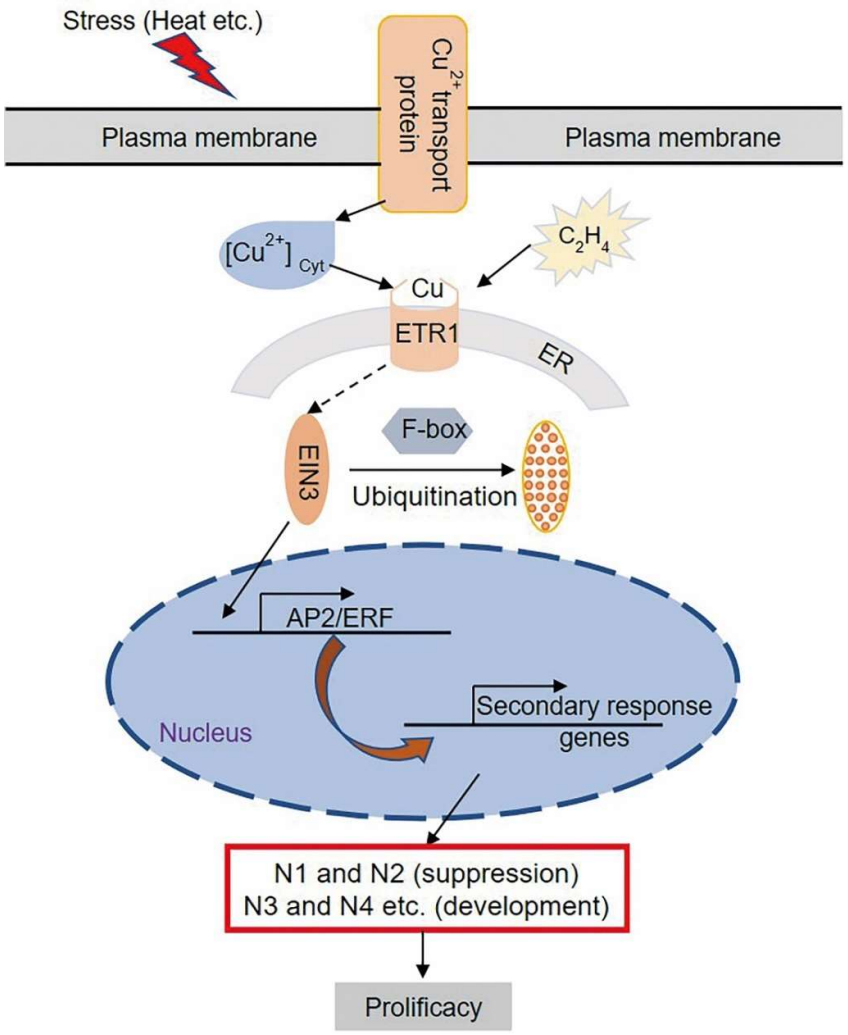

Figure 4. Model of prolificacy trait production in maize. Cyt = cytosol, ER = endoplasmic reticulum.

In the process of maize domestication, to facilitate field work and grain harvest, traditional maize tends to have fewer ears per plant to ensure maize yield. With the development of agricultural modernization, both field work and harvest can be done by machines, and maize kernels are no longer the only harvest target. This made it impossible for the currently domesticated maize to meet modern needs. With the development of science and technology, genetics, molecular breeding and other means can accelerate the breeding process of modern maize. For different harvest targets and facing different environmental stresses, the demand for ear prolificacy traits of maize is also different, so how to regulate the number of the ear is very important. The fundamental way to excavate the genes controlling the prolificacy trait and to cultivate new varieties. In previous studies, most genetic studies were carried out based on the hybrid offspring of teosinte and maize, and the gene that can affect panicle number was also cloned, such as gt1 and tb1. However, allelic variation between teosinte and maize may be too rare to be used. Combined linkage analysis and Genome-wide association study to find allelic variation that can control prolificacy traits in maize, to develop functional markers and serve molecular breeding.

 doi:10.20944/preprints202101.0185.v1

4. Materials and Methods

4.1. Material and field management

For QTL mapping analysis, two bi-parental RIL populations are generated using the method of single seed descent. One RIL population containing 276 lines was derived by crossing BT-1(low prolificacy) with XI502 (high prolificacy). The other RIL population containing 250 lines was generated by crossing N6 (low prolificacy) with CML170 (high prolificacy). The GWAS population consisted of 298 maize inbred lines, which have also been used in previous studies [42,43]. Three genetic populations were planted in Zhengzhou (ZZ: N34°44 ', E113°37 '), Xunxian (XX: N35°67 ', E114°30 '), Jiaozuo (JZ: N35°23 ', E113°53 ') and Xuchang (XC: N34° 13 ', E113°81 '), respectively. The BT-1×XI502 RIL population were planted in ZZ (in 2018, 2019 and 2020), XX (in 2018 and 2019) and XC (in 2020). The N6×CML170 RIL population were planted in XX (in 2019 and 2020), JZ (in 2019) and XC (in 2020), The GWAS populations were planted in ZZ (in 2018, 2019 and 2020), XX (in 2018 and 2019), JZ (in 2019 and 2020) and XC (in 2020). Two repeated plots were set in each environment, with a row spacing of 60cm and plant spacing of 20cm, and field management was carried out in the standard agronomic practices.

4.2. Phenotypic investigation and data analysis

After the pollen-shedding of tassel was finished, prolificacy investigation of maize was carried out, the ear with silks was considered effective, and the axillary bud which was not further developed was considered invalid. Here, we investigate the prolificacy phenomenon at different internodes to highlight the development ability of axillary buds, so the multiple ears (baby ears) at the same node were recorded as one ear. Investigate 10 plants in each row and take the average value of each material for further analysis.

Correlation analysis and frequency distribution visualization of phenotypic data in different environments of three populations were carried out with R package "Hmisc" and "PerformanceAnalytics", and AOV analysis. Genetic map construction, heritability analysis and linkage analysis were implemented with QTL IciMapping software from http://www.isbreeding.net/ [44]. The R package "LinkageMapView" is used to visualize the genetic map. Mixed linear model (MLM) of Tassal5 was used for the Genome-wide association study, in which BLUPs, markers, Kinship and PCA are included. The R package "CMplot" was used for visualization of QQ-plot and Manhattan plot. Candidate genes associated with the significant SNPs were searched by websites (www.maizeGDB.com) and screened out according to function annotations and previous research. The expression levels of candidate genes were analyzed by quantitative PCR.

4.3. RNA extraction and Quantitative Real-time PCR

The inbred lines BT-1, XI502, N6 and CML170 were planted in Zhengzhou in 2020, and the female ears of maize were sampled at different internodes during the silking period, from top to bottom namely N1, N2, N3, N4, N5 and N6, respectively. Three biological replicates were performed, and each biological replicate consisted of three samples. The Column Plant RNAout 2.0 (TIANDZ, China) was used to extract RNA from the samples. HIScript® III RT SuperMix (VazymE, China) was used for the synthesis of cDNA from the RNA samples. The primers were designed with software Primer5 (Table S1) and synthesized by the company (SunYa, China). Quantitative real-time PCR was carried out with UItraSYBR Mixture (CWBIO, China) and instrument QuantStudio5. The relative expression of candidate genes with reference to $2^{-\Delta\Delta CT}$ method to calculate.

5. Supplementary Materials:

Preprints (www.preprints.org) | NOT PEER-REVIEWED | Posted: 11 January 2021 doi:10.20944/preprints202101.0185.v1

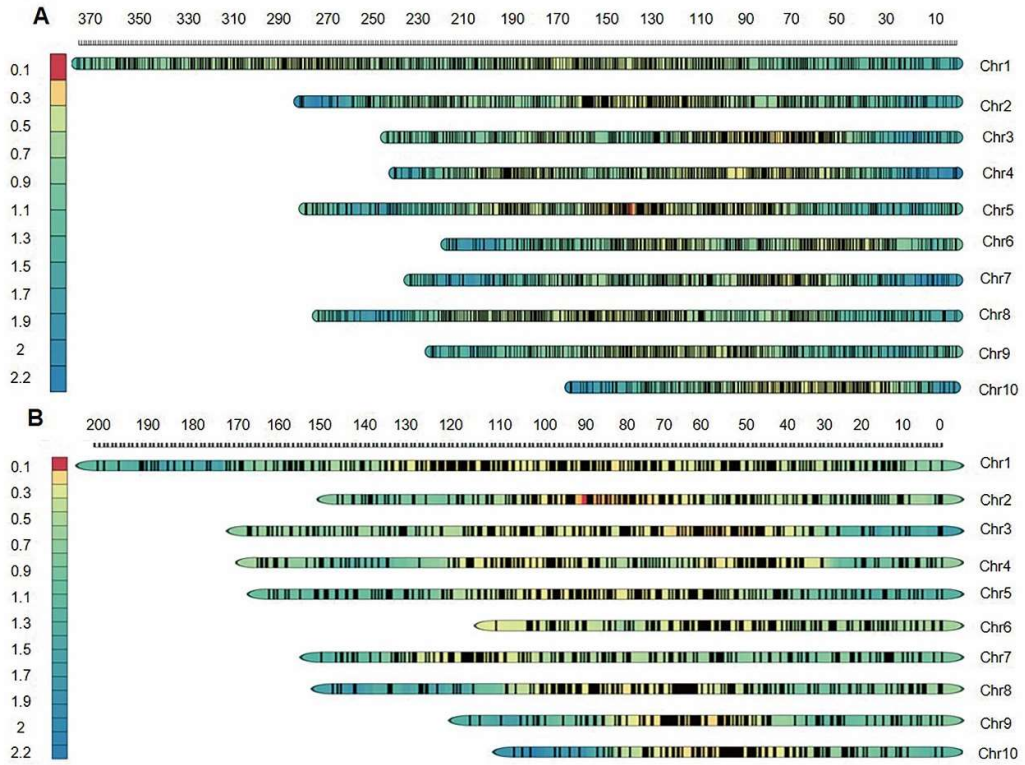

Figure S1. Genetic map of two RIL populations. A: BT-1×XI502 RIL population, B: N6×CML170 RIL population.

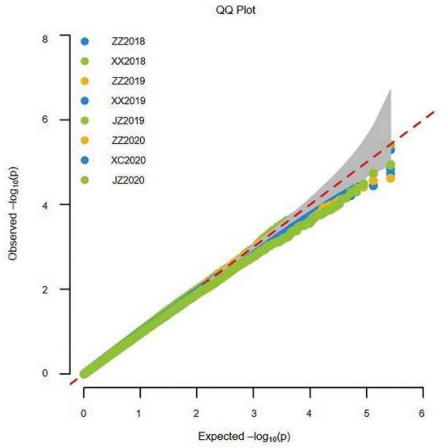

Figure S2. QQ-plots of single environment Genome Wide Association Study.

Preprints (www.preprints.org) | NOT PEER-REVIEWED | Posted: 11 January 2021 doi:10.20944/preprints202101.0185.v1

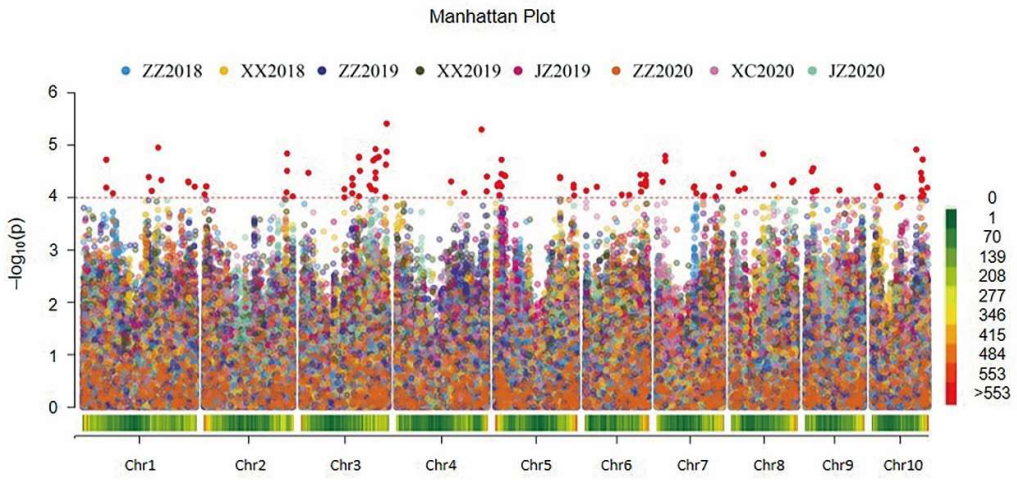

Figure S3. Manhattan plots of single environment Genome Wide Association Study. Manhattan plots. Plots above the imaginary line show the genome-wide significance with threshold of - log (10^{-4}). The horizontal axis shows the SNP density of physical positions on the ten chromosomes. The vertical axis shows the value of - log (P).

Table S1. Primers of Quantitative Real-time PCR.

Gene ID	Primer
GRMZM5G882364	F: 5'-CAGCTGCTCCATAATGTAGAGA-3'
	R: 5'-CTATCCGCTCGATCGTACATAC-3'
GRMZM2G317262	F: 5'-GAGATGAACGGCTTCTAGTCTC-3'
	R: 5'-CTGAGGCTAAAACCAACGGAG-3'
GRMZM2G317584	F: 5'-TAGCAAGTGGGAGATAAACAGG-3'
	R: 5'-ACAAGAACTGGGAAGCATAGAA-3'
GRMZM2G141679	F: 5'-CGAGGTAAGCTTAGATCTGAGC-3'
	R: 5'-GAAGAGGATGAGAGAGTCGAAG-3'
House-keeping gene	F: 5'-TGGGCCTACTGGTCTTACTACTGA-3'
	R: 5'-ACATACCCACGCTTCAGATCCT-3'

Table S2. Single environment linkage analysis of BT×XI502RIL population.

Preprints (www.preprints.org) | NOT PEER-REVIEWED | Posted: 11 January 2021 doi:10.20944/preprints202101.0185.v1

TraitName	Chromosome	LeftMarker	RightMarker	LOD	PVE(%)	Add
ZZ2018	1	1_292993929	1_293224853	7.12	5.87	0.19
ZZ2018	2	2_829447	2_1552223	6.18	5.00	0.17
ZZ2018	2	2_7267715	2_7418226	8.94	7.55	-0.21
ZZ2018	2	2_49334664	2_49460777	3.93	3.19	-0.14
ZZ2018	3	3_31245435	3_33106545	7.23	6.13	-0.19
ZZ2018	3	3_169013130	3_169083576	8.07	6.79	0.21
ZZ2018	6	6_74712832	6_75660864	4.97	3.99	-0.15
ZZ2018	9	9_139475295	9_140061322	6.75	5.71	-0.18
XX2018	2	2_26784393	2_28748530	9.72	14.57	-0.18
XX2018	6	6_98894663	6_99234929	3.76	5.24	-0.11
XX2018	9	9_135605559	9_136370952	5.58	8.15	-0.14
ZZ2019	1	1_4402935	1_4907459	3.86	6.39	0.12
ZZ2019	2	2_7653174	2_8221754	5.79	9.47	-0.15
ZZ2019	6	6_97811789	6_98272410	2.92	4.65	-0.10
ZZ2019	9	9_138556752	9_138757556	2.87	4.50	-0.10
XX2019	2	2_62770243	2_64743707	6.06	8.76	-0.11
XX2019	5	5_2388407	5_2442032	3.44	4.83	-0.09
XX2019	6	6_108448141	6_108674753	3.54	5.03	-0.09
XX2019	7	7_9820593	7_9992337	2.90	4.16	-0.08
XX2019	7	7_177668009	7_178049575	3.88	5.55	-0.09
ZZ2020	2	2_6635220	2_6961027	6.21	6.54	-0.13
ZZ2020	2	2_55426207	2_55606653	8.07	8.61	-0.15
ZZ2020	5	5_60304719	5_60955807	3.51	3.65	0.10
ZZ2020	5	5_172004071	5_172413289	6.87	7.44	-0.14
ZZ2020	6	6_4325255	6_4692158	3.16	3.47	-0.10
XC2020	1	1_297383016	1_297386460	4.17	5.31	0.17
XC2020	2	2_40140355	2_40260911	11.16	15.20	-0.28
XC2020	4	4_15450682	4_15939816	4.00	5.19	0.17
XC2020	6	6_31727950	6_32910462	3.23	4.13	-0.15
XC2020	8	8_105394925	8_105776970	2.93	3.85	0.14

Table S3. Single environment linkage analysis of N6×CML170RIL population.

Preprints (www.preprints.org) | NOT PEER-REVIEWED | Posted: 11 January 2021 doi:10.20944/preprints202101.0185.v1

TraitName	Chromosome	LeftMarker	RightMarker	LOD	PVE(%)	Add
XX2019	1	22965625	24963234	4.37	6.03	0.11
XX2019	8	128530058	131550621	3.90	5.45	-0.10
XX2019	10	80064013	80253047	7.32	10.20	0.15
JZ2019	1	202894899	203219520	8.73	4.63	0.15
JZ2019	1	201510284	202298178	15.31	8.45	-0.21
JZ2019	3	35963455	39661884	4.58	2.32	0.11
XC2020	1	21009283	22742958	4.33	4.75	0.17
XC2020	9	135295686	136357845	2.60	2.91	0.14
XX2020	1	29153532	29871226	3.64	6.00	0.14
XX2020	7	177581799	179421250	2.72	4.39	-0.12
XX2020	9	135295686	136357845	3.24	5.45	0.13

Table S4. Significant SNP and gene functional annotation of Single environment Genome-wide association study.

	Position	P	R^2	Gene	Annotation
ZZ2018	5_16844145	1.90E-05	0.09	GRMZM2G077828	(ATCNGC7, CNGC7) cyclic nucleotide gated channel 7
	5_16844539	3.54E-05	0.09	GRMZM5G838285	(ATNCED9, NCED9) nine-cis-epoxycarotenoid dioxygenase 9
ZZ2018	6_146820802	3.69E-05	0.11	GRMZM2G026523	Major facilitator superfamily protein
				GRMZM2G322220	Major facilitator superfamily protein
ZZ2018	5_23573562	3.72E-05	0.09	GRMZM2G074543	Plant-specific transcription factor YABBY family protein
ZZ2018	7_100241077	6.13E-05	0.08	GRMZM2G141679	Integrase-type DNA-binding superfamily protein
	7_100241078	6.13E-05	0.08		
	7_100241083	6.13E-05	0.08		
	7_100241087	6.13E-05	0.08		
ZZ2018	1_297745240	6.17E-05	0.09	GRMZM2G016738	nuclear antigen
				GRMZM2G016290	RmlC-like cupins superfamily protein
				GRMZM2G016084	Nucleic acid-binding proteins superfamily
				GRMZM2G316148	expressed protein
ZZ2018	6_31649694	6.29E-05	0.10	GRMZM2G025959	Mannose-binding lectin superfamily protein
ZZ2018	7_98379306	6.55E-05	0.09	none	
ZZ2018	5_207994257	6.56E-05	0.08	GRMZM2G158854	Mitochondrial transcription termination factor family protein
				GRMZM2G158848	none
				GRMZM5G862663	none
				GRMZM2G012399	S-adenosyl-L-methionine-dependent methyltransferases superfamily protein
				GRMZM2G012269	(MUB6) membrane-anchored ubiquitin-fold protein 6
				AC196008.1_FG004	expressed protein
ZZ2018	9_91476300	7.24E-05	0.10	GRMZM2G074233	serine-rich protein-related
ZZ2018	7_105366282	8.27E-05	0.08	GRMZM2G122780	expressed protein
				GRMZM2G476685	CYCLIN D1
ZZ2018	1_80621619	8.31E-05	0.09	GRMZM2G087063	(CCB2, HCF208) Protein of unknown function (DUF2930)
	1_80621624	8.31E-05	0.09	GRMZM2G703658	none

Preprints (www.preprints.org) | NOT PEER-REVIEWED | Posted: 11 January 2021 doi:10.20944/preprints202101.0185.v1

ZZ2018	5_209742952	9.15E-05	0.08	GRMZM2G101613	(ICK6, KRP3) inhibitor/interactor with cyclin-dependent kinase
				GRMZM2G163776	expressed protein
XX2018	1_200725159	1.11E-05	0.12	GRMZM2G152156	root cap 1 (RCP1)
				GRMZM2G133413	Cyclin D2
XX2018	8_85309063	1.47E-05	0.10	GRMZM2G044997	(ATRTL2, RTL2) RNAse THREE-like protein 2
XX2018	9_17667914	3.16E-05	0.09	GRMZM2G429378	(CRF4) cytokinin response factor 4
				GRMZM2G071249	GDSL-like Lipase/Acylhydrolase superfamily protein
XX2018	10_132512165	4.27E-05	0.08	GRMZM2G040902	(ATSYP81, ATUFE1, SYP81, UFE1) syntaxin of plants 81
				GRMZM2G040803	zinc finger C3HC4 type domain containing protein expressed
	10_132527539	4.59E-05	0.08	GRMZM2G468661	(GATL4) galacturonosyltransferase-like 4
				GRMZM2G468688	expressed protein
				GRMZM2G468693	Aldolase-type TIM barrel family protein
				GRMZM2G468756	lectin-like receptor kinase
				GRMZM2G168953	reductase family domain containing protein
XX2018	1_280826399	5.14E-05	0.12	GRMZM2G072814	none
				GRMZM2G072682	clast3-related
				GRMZM2G072653	(AOS, CYP74A, DDE2) allene oxide synthase
				GRMZM2G376668	none
XX2018	5_207892023	5.69E-05	0.09	GRMZM2G320786	(LAC14) laccase 14
				GRMZM2G017355	Mitochondrial transcription termination factor family protein
				GRMZM2G017429	Mitochondrial transcription termination factor family protein
				AC196008.1_FG001	none
XX2018	3_181559598	5.91E-05	0.09	GRMZM5G871592	Domain of unknown function (DUF966)
				GRMZM2G376061	C2H2-type zinc finger family protein
				GRMZM5G804618	C2H2 and C2HC zinc fingers superfamily protein
				GRMZM5G843352	none
				GRMZM2G436295	none
XX2018	2_7178420	6.15E-05	0.11	GRMZM2G115716	S-locus lectin protein kinase family protein
	2_7178428	6.15E-05	0.11	GRMZM2G115705	(ARK3, RK3) receptor kinase 3
				GRMZM2G115598	eukaryotic translation initiation factor 3C
XX2018	3_114779132	6.94E-05	0.08	GRMZM2G059703	none
				GRMZM2G368126	Transducin/WD40 repeat-like superfamily protein
				GRMZM2G046841	(H2B, HTB9) Histone superfamily protein
XX2018	10_132424212	7.32E-05	0.08	GRMZM2G046841	(H2B, HTB9) Histone superfamily protein
XX2018	2_219022778	7.93E-05	0.08	GRMZM2G169681	(BAM1) Leucine-rich receptor-like protein kinase family protein
	2_219022780	7.93E-05	0.08		
XX2018	10_23072865	9.01E-05	0.08	GRMZM2G058612	F-box family protein
XX2018	3_153915505	9.44E-05	0.08	GRMZM2G145814	alpha/beta-Hydrolases superfamily protein
				GRMZM2G145715	6-phosphogluconate dehydrogenase family protein
				GRMZM2G145709	Protein kinase superfamily protein
XX2018	3_114782746	9.83E-05	0.09	GRMZM2G059703	none
				GRMZM2G368126	Transducin/WD40 repeat-like superfamily protein

Preprints (www.preprints.org) | NOT PEER-REVIEWED | Posted: 11 January 2021 doi:10.20944/preprints202101.0185.v1

ZZ2019	10_118146700	1.21E-05	0.11	GRMZM2G045280	Coiled-coil domain-containing protein 55 (DUF2040)
				GRMZM2G139419	(ATUPF3, UPF3) Smg-4/UPF3 family protein
ZZ2019	10_134970131	1.87E-05	0.10	GRMZM2G097813	NB-ARC domain-containing disease resistance protein
				GRMZM2G097848	(MCD1) multiple chloroplast division site 1
ZZ2019	10_130205182	3.37E-05	0.08	GRMZM2G160069	(ATINT4, INT4) inositol transporter 4
				GRMZM5G866420	none
				GRMZM2G016487	RING/U-box superfamily protein
ZZ2019	1_175591561	4.06E-05	0.10	none	
ZZ2019	5_172396840	4.11E-05	0.08	GRMZM2G006791	(TAPX) thylakoidal ascorbate peroxidase
	5_172396964	4.14E-05	0.08		
	5_172396661	4.24E-05	0.08		
ZZ2019	3_136085076	4.29E-05	0.09	GRMZM2G092142	none
	3_136085124	4.29E-05	0.09	GRMZM2G092169	Protein of Unknown Function (DUF239)
	3_136094461	8.30E-05	0.09		
	3_136094478	8.30E-05	0.09		
	3_136094448	8.30E-05	0.09		
ZZ2019	3_136337629	5.73E-05	0.08	GRMZM2G019090	(ATGSTZ2, GSTZ2) glutathione S-transferase (class zeta) 2
	3_136336358	5.80E-05	0.08		
ZZ2019	6_3042472	7.36E-05	0.07	GRMZM2G374827	Beta-glucosidase GBA2 type family protein
				GRMZM2G073521	none
				GRMZM2G073495	Ribosomal protein L19 family protein
ZZ2019	10_130286132	9.69E-05	0.08	GRMZM2G154721	GC-rich sequence DNA-binding factor-like protein with Tuftelin interacting domain
				GRMZM2G154725	expressed protein
				GRMZM5G810727	(BGLU47) beta-glucosidase 47
				GRMZM2G031628	(BGLU47) beta-glucosidase 47
				GRMZM2G031660	(BGLU46) beta glucosidase 46
XX2019	4_226006703	5.04E-06	0.11	GRMZM2G004741	(GTE4) global transcription factor group E4
				GRMZM2G100234	Protein kinase family protein with leucine-rich repeat domain
XX2019	3_153915506	1.65E-05	0.11	GRMZM2G145814	alpha/beta-Hydrolases superfamily protein
	3_153915511	1.65E-05	0.11	GRMZM2G145715	6-phosphogluconate dehydrogenase family protein
	3_153915508	1.72E-05	0.11	GRMZM2G145709	Protein kinase superfamily protein
XX2019	3_205804664	1.69E-05	0.09	AC233882.1_FG005	(ATKCO2, ATTPK2, KCO2) Ca2+ activated outward rectifying K+ channel 2
				GRMZM5G829563	expressed protein
XX2019	1_63098589	1.89E-05	0.10	GRMZM2G046297	Protein kinase superfamily protein
				GRMZM2G109126	none
				GRMZM5G801004	none
XX2019	3_155968195	3.10E-05	0.09	GRMZM2G161380	Protein kinase superfamily protein
				GRMZM2G161295	(NDH18) NAD(P)H dehydrogenase 18
XX2019	8_6111245	3.51E-05	0.08	GRMZM2G044819	HAD-superfamily hydrolase subfamily IG 5\'-nucleotidase
				GRMZM2G010280	(ATNRT2.4, NRT2.4) nitrate transporter 2.4
				AC183888.4_FG006	(ATH9, TH9, TRX H9) thioredoxin H-type 9
XX2019	4_240254055	3.97E-05	0.09	GRMZM2G010251	nitrate transporter 2:1
	4_240254058	3.97E-05	0.09	GRMZM2G010163	none

Preprints (www.preprints.org) | NOT PEER-REVIEWED | Posted: 11 January 2021 doi:10.20944/preprints202101.0185.v1

				GRMZM2G010091	(WAK2) wall-associated kinase 2
XX2019	1_280560002	4.91E-05	0.09	GRMZM2G353114	(ELF9) RNA binding (RRM/RBD/RNP motifs) family protein
				GRMZM2G037617	(AtAUR3, AUR3) ataurora3
				GRMZM2G345582	hydroxyproline-rich glycoprotein family protein
				GRMZM2G009944	none
				GRMZM2G009958	(MEE14) maternal effect embryo arrest 14
XX2019	4_145545079	4.94E-05	0.09	GRMZM2G111225	(AtNIT4, NIT4) nitrilase 4
XX2019	10_12924816	6.03E-05	0.08	GRMZM2G015869	PQ-loop repeat family protein / transmembrane family protein
XX2019	2_6031628	6.09E-05	0.08	GRMZM2G023071	Pentatricopeptide repeat (PPR) superfamily protein
				GRMZM2G023037	(ATCNGC8, CNGC8) cyclic nucleotide gated channel 8
				GRMZM2G022836	2-oxoglutarate (2OG) and Fe(II)-dependent oxygenase superfamily protein
				GRMZM2G022563	(KAS III) 3-ketoacyl-acyl carrier protein synthase III
				GRMZM2G022192	Amidase family protein
				GRMZM2G021635	proton pump D subunit (VATPD)
XX2019	7_165754293	6.17E-05	0.08	GRMZM2G054032	F-box family protein
				GRMZM2G053999	(ALAAT2) alanine aminotransferase 2
				GRMZM2G053939	(ALAAT2) alanine aminotransferase 2
XX2019	1_63098599	6.49E-05	0.09	GRMZM2G109126	none
				GRMZM2G046297	Protein kinase superfamily protein
				GRMZM5G801004	none
XX2019	7_126222900	9.12E-05	0.08	GRMZM2G096271	Calcium-binding EF-hand family protein
				AC202417.5_FG002	none
				GRMZM2G090739	expressed protein
JZ2019	3_227048455	3.87E-06	0.13	GRMZM2G064031	Heat shock protein DnaJ N-terminal with domain of unknown function
	3_227051329	1.34E-05	0.11		
JZ2019	5_27053405	3.86E-05	0.09	GRMZM2G162544	(ATSYP43, SYP43) syntaxin of plants 43
				GRMZM2G117963	Peptide-N4-(N-acetyl-beta-glucosaminyl) asparagine amidase A protein
JZ2019	7_15828044	5.00E-05	0.10	GRMZM2G478965	(ATERF1, ERF1) ethylene response factor 1
JZ2019	5_11798566	5.26E-05	0.09	GRMZM2G024973	(RGA, RGA1) GRAS family transcription factor family protein
				GRMZM2G024690	Transmembrane Fragile-X-F-associated protein
JZ2019	5_5622757	5.99E-05	0.10	GRMZM2G091535	Seed maturation protein
				AC205490.4_FG004	none
				GRMZM2G091527	(ANT, CKC, CKC1, DRG) Integrase-type DNA-binding superfamily protein
				GRMZM2G386273	bZIP transcription factor domain containing protein
				GRMZM2G534096	none
				GRMZM2G091487	Carbohydrate-binding protein
JZ2019	5_17115812	6.04E-05	0.08	GRMZM2G095239	(ATTRB1, TRB1) telomere repeat binding factor 1
JZ2019	1_183779929	7.43E-05	0.08	GRMZM2G113127	(ATHAP5B, HAP5B, NF-YC2) nuclear factor Y subunit C2
				GRMZM2G113196	expressed protein
				GRMZM2G113229	(ATRD22, RD22) BURP domain-containing protein
				GRMZM2G113726	Transducin/WD40 repeat-like superfamily protein
JZ2019	9_20324957	7.67E-05	0.10	GRMZM2G106683	(SOL1) carboxypeptidase D putative
	9_20324985			GRMZM2G444801	(SULTR3;4) sulfate transporter 3

Preprints (www.preprints.org) | NOT PEER-REVIEWED | Posted: 11 January 2021 doi:10.20944/preprints202101.0185.v1

	9_20324986				
JZ2019	10_136707307	8.78E-05	0.08	GRMZM2G077082	(TBL11) TRICHOME BIREFRINGENCE-LIKE 11
				GRMZM2G077069	(AtPP2-A13, PP2-A13) phloem protein 2-A13
				GRMZM2G077036	S-adenosyl-L-methionine-dependent methyltransferases superfamily protein
JZ2019	5_11490848	8.99E-05	0.08	GRMZM2G177942	(AHP2) Arabidopsis Hop2 homolog
				GRMZM2G177934	(ARPN) plantacyanin
				GRMZM2G177885	zinc finger (Ran-binding) family protein
JZ2019	7_156495795	9.60E-05	0.07	GRMZM2G309025	S-locus lectin protein kinase family protein
				GRMZM2G008740	expressed protein
	7_156495832	9.60E-05	0.07	GRMZM2G008687	PLAC8 family protein
				GRMZM2G008528	OsFBX250 - F-box domain containing protein expressed
JZ2019	10_80573093	9.85E-05	0.08	GRMZM2G333183	(ABCB1, ATPGP1, PGP1) ATP binding cassette subfamily B1
				GRMZM2G446895	ARM repeat superfamily protein
				GRMZM2G502467	none
ZZ2020	5_172293904	1.83E-05	0.14	GRMZM2G139035	none
				GRMZM2G139031	(ATOGG1, OGG1) 8-oxoguanine-DNA glycosylase 1
ZZ2020	6_161243424	1.13E-05	0.12	GRMZM2G158972	DNAse I-like superfamily protein
	6_161243515	5.71E-05	0.12	GRMZM2G159008	DNAse I-like superfamily protein
	6_161283893	2.41E-05	0.12	GRMZM2G159032	(ATHD2A, HD2A, HDA3, HDT1) histone deacetylase 3
	6_161283910	2.70E-05	0.11	GRMZM2G159404	UDP-Glycosyltransferase superfamily protein
	6_161280391	4.14E-05	0.10	GRMZM2G460542	(ATESD4, ESD4) Cysteine proteinases superfamily protein
				GRMZM2G034225	expressed protein
ZZ2020	3_225226430	4.51E-05	0.09	GRMZM2G001296	(MEE18) maternal effect embryo arrest 18
				GRMZM2G483804	none
				GRMZM2G049866	RNA-binding (RRM/RBD/RNP motifs) family protein
ZZ2020	9_21997264	4.78E-05	0.11	none	
ZZ2020	6_148593356	8.06E-05	0.09	GRMZM2G033641	phosphoglyceride transfer family protein
ZZ2020	1_85018362	9.06E-05	0.10	GRMZM5G837538	none
				GRMZM2G026147	expansin-like A1
				GRMZM2G327907	expressed protein
ZZ2020	9_89811263	9.08E-05	0.09	GRMZM2G041831	Mitochondrial substrate carrier family protein
				GRMZM2G342738	expressed protein
XC2020	6_117453528	3.62E-05	0.10	GRMZM2G168304	(CER6, CUT1, G2, KCS6, POP1) 3-ketoacyl-CoA synthase 6
XC2020	6_97345203	4.25E-05	0.10	GRMZM2G322866	expressed protein
				GRMZM2G018105	GDSL-like Lipase/Acylhydrolase superfamily protein
				GRMZM2G018280	(HT1) Protein kinase superfamily protein
XC2020	4_234572427	4.61E-05	0.10	GRMZM2G304712	(UGT84A1) UDP-Glycosyltransferase superfamily protein
				GRMZM2G008859	translocon at inner membrane of chloroplasts 21
XC2020	9_154025190	7.89E-05	0.09	AC196090.3_FG006	(SDD1) Subtilase family protein
				GRMZM2G106263	3-hydroxy-3-methylglutaryl coenzyme A synthase
XC2020	7_124212594	7.28E-05	0.09	GRMZM2G151299	expressed protein
	7_124212655	7.92E-05	0.09	GRMZM2G121649	Microtubule associated protein (MAP65/ASE1) family protein
	7_124212630	7.96E-05	0.09		

 doi:10.20944/preprints202101.0185.v1

XC2020	3_225119653	8.27E-05	0.11	GRMZM2G002578 GRMZM2G022279	DnaJ/Hsp40 cysteine-rich domain superfamily protein GDSL-like Lipase/Acylhydrolase superfamily protein
JZ2020	3_197320947	2.83E-05	0.10	GRMZM2G021704	(DHOASE, PYR4) pyrimidin 4
	3_197320911	4.25E-05	0.11	GRMZM2G317285	Tetratricopeptide repeat (TPR)-like superfamily protein
	3_197321346	8.86E-05	0.10		
JZ2020	2_235853396	7.27E-05	0.10	GRMZM2G148693	K-box region and MADS-box transcription factor family protein

6. Author Contributions:

Jianyu Wu, Zhao Wang, Zijian Zhou, Jiafa Chen and Jingyang Gao designed the experiments and wrote the manuscript. Zhao Wang, Yunmeng Li, Jingyang Gao, Yifan Luan, Cong Mu, Chaopei Dong, Yunxia Song, Jing Xu, Zhaokun Wu, Wenchao Ye and Huan Li performed the experiments. Zhao Wang, Jingyang Gao, and Zijian Zhou analyzed data. Razia sultana Jemim and Haidong Yu participated in revising the article.

Funding: This research received no external funding.

Acknowledgments: This work was financially supported by the Co-construction State Key Laboratory of Wheat and Crop Science of China.

Conflicts of Interest: The authors have no conflicts of interest to disclose in the authorship and publication of this document.

References

1. Hake, S.; Richardson, A. Using wild relatives to improve maize. *Science* **2019**, *365*, 640-641, doi:10.1126/science.aay5299.
2. Wills, D.M.; Whipple, C.J.; Takuno, S.; Kursel, L.E.; Shannon, L.M.; Ross-Ibarra, J.; Doebley, J.F. From many, one: genetic control of prolificacy during maize domestication. *PLoS Genet* **2013**, *9*, e1003604, doi:10.1371/journal.pgen.1003604.
3. Premlatha, M.; Kalamani, A. Heterosis and combining ability studies for grain yield and its related traits in maize (Zea mays L.). *Mysore Journal of Agricultural Sciences* **2009,** *43*, 62-66, doi:10.5958/0975-928x.2018.00126.6.
4. Silva, I.G.D.; Castoldi, R.; Charlo, H.C.d.O.; Miranda, M.D.S.; Lemes, E.M. Prediction of genetic gain in sweet corn using selection indexes. *Journal of Crop Science and Biotechnology* **2020**, *23*, 191-196, doi:10.1007/s12892-019-0334-0.
5. Kir, H. Yield and quality traits of some silage maize cultivars. *Fresenius Environmental Bulletin* **2020**, *29*, 2843-2849.
6. Matsuoka, Y.; Vigouroux, Y.; Goodman, M.M.; Sanchez, G.J.; Buckler, E.; Doebley, J. A single domestication for maize shown by multilocus microsatellite genotyping. *Proc Natl Acad Sci U S A* **2002**, *99*, 6080-6084, doi:10.1073/pnas.052125199.
7. Doebley, J. The genetics of maize evolution. *Annu Rev Genet* **2004**, *38*, 37-59, doi:10.1146/annurev.genet.38.072902.092425.
8. Iltis, H.H. From teosinte to maize: the catastrophic sexual transmutation. *Science* **1983**, *222*, 886-894, doi:10.1126/science.222.4626.886.
9. Lejeune, P.; Bernier, G. Effect of environment on the early steps of ear initiation in maize (Zea mays L.). *Plant, Cell & Environment* **1996**, *19*,217-224, doi:10.1111/j.1365-3040.1996.tb00243.x.
10. Domagalska, M.A.; Leyser, O. Signal integration in the control of shoot branching. *Nature reviews. Molecular cell biology* **2011**, *12*, 211-221, doi:10.1038/nrm3088.
11. Dong, Z.; Xiao, Y. The regulatory landscape of a core maize domestication module controlling bud dormancy and growth repression. *Nature communications* **2019**, *10*, 3810, doi:10.1038/s41467-019-11774-w.
12. Al-Naggar, A.M.M.; Shabana, R.; Rabie, A.M. Inheritance of maize prolificacy under high plant density. *Egyptian Journal of Plant Breeding* **2012**, *16*, 1-27, doi:10.12816/0003929.
13. Anderson; E.; L.; Kamprath; E.; J.; Moll; R.; H. Prolificacy and N fertilizer effects on yield and N utilization in maize[1]. *Crop Science* **1985,** *25*, 598-602, doi:10.2135/cropsci1985.0011183X002500040005x.

14. Zhu, Y.; Fu, J.; Zhang, J.; Liu, T.; Jia, Z.; Wang, J.; Jin, Y.; Lian, Y.; Wang, M.; Zheng, J. Genome-wide analysis of gene expression profiles during ear development of maize. *Plant Molecular Biology* **2009**, *70*, 63-77, doi:10.1007/s11103-009-9457-2.
15. Nemhauser, J.L.; Feldman, L.J.; Zambryski, P.C. Auxin and ETTIN in Arabidopsis gynoecium morphogenesis. *Development* **2000**, *127*, 3877-3888, PMID:10952886.
16. Faiss, M.; Zalubìlová, J.; Strnad, M.; Schmülling, T. Conditional transgenic expression of the ipt gene indicates a function for cytokinins in paracrine signaling in whole tobacco plants. *The Plant journal : for cell and molecular biology* **1997**, *12*, 401-415, doi:10.1046/j.1365-313x.1997.12020401.x.
17. Müller, D. Auxin, cytokinin and the control of shoot branching. *Ann Bot* **2011**, *107*, 1203-1212, doi:10.1093/aob/mcr069.
18. González-Grandío, E.; Pajoro, A.; Franco-Zorrilla, J.M.; Tarancón, C.; Immink, R.G.; Cubas, P. Abscisic acid signaling is controlled by a BRANCHED1/HD-ZIP I cascade in Arabidopsis axillary buds. Proc Natl Acad Sci U S A **2017**, *114*, E245, doi:10.1073/pnas.1613199114.
19. Wang, B.; Smith, S.M.; Li, J. Genetic regulation of shoot architecture. *Annual Review of Plant Biology* **2018**, *69*, 473-468.
20. Francis, D.; Halford, N.G. Nutrient sensing in plant meristems. *Plant Molecular Biology* **2006**, *60*, 981-993, doi:10.1146/annurev-arplant-042817-040422.
21. Wu, X.; Dabi, T.; Weigel, D. Requirement of homeobox gene STIMPY/WOX9 for Arabidopsis meristem growth and maintenance. *Current Biology* **2005**, *15*, 436-440, doi:10.1016/j.cub.2004.12.079.
22. Satohnagasawa, N.; Nagasawa, N.; Malcomber, S.T.; Sakai, H.; Jackson, D. A trehalose metabolic enzyme controls inflorescence architecture in maize. *Nature* **2006**, *441*, 227-230, doi:10.1038/nature04725.
23. Urano, D.; Jackson, D.; Jones, A.M. A G protein alpha null mutation confers prolificacy potential in maize. *Journal of Experimental Botany* **2015**, *66*, 4511-4515, doi:10.1093/jxb/erv215.
24. Prakash, N.R.; Zunjare, R.U.; Muthusamy, V.; Chand, G.; Hossain, F. Genetic analysis of prolificacy in "Sikkim Primitive"—A prolific maize (Zea mays) landrace of North-Eastern Himalaya. *Plant Breeding* **2019,** *138,* 781-789, doi:10.1111/pbr.12736.
25. Whipple, C.J.; Kebrom, T.H.; Weber, A.L.; Yang, F.; Hall, D.; Meeley, R.; Schmidt, R.; Doebley, J.; Brutnell, T.P.; Jackson, D.P. Grassy tillers1 promotes apical dominance in maize and responds to shade signals in the grasses. *Proceedings of the National Academy of Sciences* **2011**, *108*, E506-E512, doi:10.1073/pnas.1102819108.
26. Doebley, J.; Stec, A.O.; Hubbard, L. The evolution of apical dominance in maize. *Nature* **1997**, *386*, 485-488, doi:10.1038/386485a0.
27. Studer, A.; Zhao, Q.; Ross-Ibarra, J.; Doebley, J. Identification of a functional transposon insertion in the maize domestication gene tb1. *Nature Genetics* **2011**, *43*, 1160-1663, doi:10.1038/ng.942.
28. Doebley, J.; Stec, A.; Gustus, C. Teosinte branched1 and the origin of maize: evidence for epistasis and the evolution of dominance. *Genetics* **1995**, *141*, 333-346.
29. Liu, H.; Qin, C.; Chen, Z.; Zuo, T.; Pan, G. Identification of miRNAs and their target genes in developing maize ears by combined small RNA and degradome sequencing. *Bmc Genomics* **2014**, *15*, 25, doi:10.1186/1471-2164-15-25.
30. Leon, D.; N.; Coors; J., O.; Kaeppler; S., M.; Rosa; G., J.M. Genetic control of prolificacy and Related Traits in the Golden Glow Maize Population: I. Phenotypic Evaluation. *Crop Science* **2005,** *45,* 1361-1369, doi:10.2135/cropsci2003.0486.
31. Jian-Ping, A.; Xiao-Fei, W.; Yuan-Yuan, L.; Lai-Qing, S.; Ling-Ling, Z.; Chun-Xiang, Y.; Yu-Jin, H. EIN3-LIKE1, MYB1, and ETHYLENE RESPONSE FACTOR3 act in a regulatory loop that synergistically modulates ethylene biosynthesis and anthocyanin accumulation. *Plant Physiology* **2018**, *178,* 808-823, doi:10.1104/pp.18.00068.
32. Liu, C.; Li, J.; Zhu, P.; Yu, J.; Hou, J.; Wang, C.; Long, D.; Yu, M.; Zhao, A. Mulberry EIL3 confers salt and drought tolerances and modulates ethylene biosynthetic gene expression. *PeerJ* **2019**, *7*, e6391, doi:10.7717/peerj.6391.

33. Yi-Qin, H.; Wen-Di, H.; Lei, Y.; Yi-Ting, L.; Jun-Liang, Y. Genome-wide analysis of ethylene-insensitive3 (EIN3/EIL) in Triticum aestivum. *Crop ence* **2020,** *60*, 2019-2037, doi:10.1002/csc2.20115.
34. Zhao, M.; Liu, W.; Xia, X.; Wang, T.; Zhang, W.H. Cold acclimation-induced freezing tolerance of Medicago truncatula seedlings is negatively regulated by ethylene. *Physiologia Plantarum* **2014**, *152*, 115-129, doi:10.1111/ppl.12161.
35. Shi, Y.; Tian, S.; Hou, L.; Huang, X.; Zhang, X.; Guo, H.; Yang, S. Ethylene Signaling Negatively Regulates Freezing Tolerance by Repressing Expression of CBF and Type-A ARR Genes in Arabidopsis. *Plant Cell* **2012**, *24*, 2578-2595, doi:10.1105/tpc.112.098640.
36. Ciaffi, M.; Paolacci, A.R.; D"Aloisio, E.; Tanzarella, O.A.; Porceddu, E. Identification and characterization of gene sequences expressed in wheat spikelets at the heading stage. *Gene* **2005**, *346*, 221-230, doi:10.1016/j.gene.2004.11.004.
37. Vierstra, R.D. The ubiquitin/26S proteasome pathway, the complex last chapter in the life of many plant proteins. *Trends in Plant ence* **2003**, *8*, 135-142, doi:10.1016/S1360-1385(03)00014-1.
38. Zhang, X.; Gonzalez-Carranza, Z.H.; Zhang, S.; Miao, Y.; Roberts, J.A. *F-Box Proteins in Plants*. *Annual Plant Reviews online*. **2019**, *2*, 1-21, doi:10.1002/9781119312994.apr0701.
39. An, F.; Zhao, Q.; Ji, Y.; Li, W.; Jiang, Z.; Yu, X.; Zhang, C.; Han, Y.; He, W.; Liu, Y. Ethylene-Induced stabilization of ETHYLENE INSENSITIVE3 and EIN3-LIKE1 is mediated by proteasomal degradation of EIN3 binding F-Box 1 and 2 that requires EIN2 in Arabidopsis. *Plant Cell* **2010**, *22*, 2384-2401, doi:10.1105/tpc.110.076588.
40. Yruela Guerrero, I. Copper in plants: acquisition, transport and interactions. *Functional Plant Biology* **2009**, *36*, 409-430, doi:10.1071/FP08288.
41. Rodr; iacute; Guez, F.I. A copper cofactor for the ethylene receptor ETR1 from Arabidopsis. *Science* **1999**, *283*, 996-998, doi:10.1126/science.283.5404.996.
42. Zhou, B.; Zhou, Z.; Ding, J.; Zhang, X.; Mu, C.; Wu, Y.; Gao, J.; Song, Y.; Wang, S.; Ma, J. Combining three mapping strategies to reveal quantitative trait loci and candidate genes for maize ear length. *The Plant Genome* **2018**, *11*, 3, doi:10.3835/plantgenome2017.11.0107.
43. Mu, C.; Gao, J.; Zhou, Z.; Wang, Z.; Sun, X.; Zhang, X.; Dong, H.; Han, Y.; Li, X.; Wu, Y., et al. Genetic analysis of cob resistance to *F. verticillioides*: another step towards the protection of maize from ear rot. *Theoretical and applied genetics.* **2019**, *132*, 1049-1059, doi:10.1007/s00122-018-3258-4.
44. Meng, L.; Li, H.; Zhang, L.; Wang, J. QTL IciMapping: Integrated software for genetic linkage map construction and quantitative trait locus mapping in biparental populations-ScienceDirect. *The Crop Journal* **2015**, *3*, 269-283, doi:10.1016/j.cj.2015.01.001.